

Seasonal Growth and Senescence of a *Zostera marina* Seagrass Meadow Alters Wave-Dominated Flow and Sediment Suspension Within a Coastal Bay

Jennifer C. R. Hansen · Matthew A. Reidenbach

Received: 16 June 2012 / Revised: 26 February 2013 / Accepted: 22 March 2013 / Published online: 19 April 2013
© Coastal and Estuarine Research Federation 2013

Abstract Tidally driven flows, waves, and suspended sediment concentrations were monitored seasonally within a *Zostera marina* seagrass (eelgrass) meadow located in a shallow (1–2 m depth) coastal bay. Eelgrass meadows were found to reduce velocities approximately 60 % in the summer and 40 % in the winter compared to an adjacent unvegetated site. Additionally, the seagrass meadow served to dampen wave heights for all seasons except during winter when seagrass meadow development was at a minimum. Although wave heights were attenuated across the meadow, orbital motions caused by waves were able to effectively penetrate through the canopy, inducing wave-enhanced bottom shear stress (τ_b). Within the seagrass meadow, τ_b was greater than the critical stress threshold (=0.04 Pa) necessary to induce sediment suspension 80–85 % of the sampling period in the winter and spring, but only 55 % of the time in the summer. At the unvegetated site, τ_b was above the critical threshold greater than 90 % of the time across all seasons. During low seagrass coverage in the winter, near-bed turbulence levels were enhanced, likely caused by stem–wake interaction with the sparse canopy. Reduction in τ_b within the seagrass meadow during the summer correlated to a 60 % reduction in suspended sediment concentrations but in winter, suspended sediment was enhanced compared to the unvegetated site. With minimal seagrass coverage, τ_b and wave statistics were similar to unvegetated regions; however, during high seagrass coverage, sediment stabilization increased light availability for photosynthesis and created a positive feedback for seagrass growth.

Keywords Eelgrass · Seagrass · Waves · Turbulence · Sediment

Introduction

Seagrass meadows induce hydrodynamic drag on the flow that reduces water velocities and attenuates wave energy (Ackerman and Okubo 1993; Bryan et al. 2007; Carr et al. 2010; Gambi et al. 1990; Granata et al. 2001; Koch and Gust 1999; Peterson et al. 2004). These plants also serve to shelter the seafloor from hydrodynamic shear stresses (Bouma et al. 2009; Sand-Jensen 2008; Vogel 1981), which has been found to reduce the resuspension of sediments (Carr et al. 2010; Gacia and Duarte 2001; Granata et al. 2001; Ward et al. 1984). This has led to the view that seagrass meadows serve as depositional environments for sediment (Gacia et al. 1999; Gruber and Kemp 2010). Seagrasses require incident light radiation for growth (Duarte 1991); therefore, the stabilizing effect they have on sediments, and the corresponding increase in light penetration to the seafloor, creates a positive feedback for their growth (Carr et al. 2010). Since the relative amount of open space within a meadow influences the magnitude of bed shear reaching the seafloor, seagrass density can control the degree of sediment resuspension (de Boer 2007). Though meadows are often net depositional, spatial and temporal variability within seagrass meadows can create localized enhancement of sediment suspension and transport. Recent findings support a more dynamic seagrass–sediment interaction, where sediment scouring occurs on the edge of meadows (Chen et al. 2007), and low densities of seagrass can actually enhance sediment suspension (Lawson et al. 2012). This switch from an erosional to

J. C. R. Hansen (✉) · M. A. Reidenbach
Department of Environmental Sciences, University of Virginia,
Charlottesville, VA 22904, USA
e-mail: jcrhansen@virginia.edu

depositional environment may depend on the development of skimming flow over the meadow, where a shift can occur from horizontal flow diversion around individual seagrass blades in low-density seagrass systems (i.e., blades per square meter of seafloor), causing scouring around individual shoots (Nepf 1999), to vertical diversion above the meadow, reducing water velocities and turbulence adjacent to the bed within a high-density seagrass canopy (Lawson et al. 2012).

In addition to seagrass density, the magnitude of fluid shear stresses impacting the seafloor in shallow-water environments can be controlled by whether flows are dominated by tidal currents or orbital wave motion. The interaction between waves and currents is nonlinear and leads to changes in the hydrodynamics and shear stresses imposed on the seafloor from those expected under either condition independently (Jing and Ridd 1996). Luhar et al. (2010) found that seagrasses caused only minor reductions of in-canopy oscillatory motions produced by waves, in contrast to unidirectional flows that can be significantly damped within a meadow. Typically, when waves are present, a thin, oscillatory wave boundary layer develops that is more strongly sheared than one formed under steady currents alone (Grant and Madsen 1979). This wave boundary layer induces greater drag on the mean flow and increased bottom shear stresses. For waves that are typically generated in fetch-limited shallow coastal bays, wave orbital motions decrease with depth and the magnitude of wave energy that reaches the seafloor depends on the wave period, wave height, and water depth (de Boer 2007; Chen et al. 2007; Fagherazzi and Wiberg 2009). Although wave energy attenuation increases with increasing shoot density (Chen et al. 2007), the degree of flow reduction by the canopy can also be a function of distance from the edge, and the depth at which the seagrass resides below the surface (Fonseca and Fisher 1986; Verduin and Backhaus 2000). Within a *Thalassia testudinum* seagrass meadow, the density of the canopy was important in controlling mixing across the canopy–water interface (Koch and Gust 1999), and with relative increases of wave- versus tidally-driven currents, near-bed velocities and shear stresses increased. With waves, orbital motions cause the canopy to oscillate, which limits the development of skimming flows, thereby enhancing the interaction of water masses across the canopy–water interface and increasing bed shear stresses (Koch and Gust 1999).

In temperate climates, *Zostera marina* meadows typically germinate in the fall, between mid-October to November in the coastal bays of Virginia, USA (Moore et al. 1993; Orth et al. 2012), and flowering shoots mature in late spring to early summer (May–June). The meadow reaches maximum blade density and coverage midsummer, begins senescence in late summer, and has sparse coverage over the winter (Orth et al. 2012). The sloughing of leaves in the senescent

seagrass meadow effectively thins the meadow density and shortens the canopy height. Such changes to seagrass blade density and height have been shown to influence fluid velocities within meadows (Fonseca and Koehl 2006; Nepf et al. 2007), where canopy friction exhibits a strong positive relationship to the percent of the water column that is occupied by the seagrass (Fonseca and Fisher 1986). In Gacia and Duarte (2001), resuspension of sediment was greatest with minimum canopy development, while deposition occurred under maximum above-ground canopy biomass conditions. Studies also show that mixing rates and turbulent kinetic energy are highly dependent upon seagrass density and areal cover of the canopy (Granata et al. 2001; Hansen and Reidenbach 2012). These findings suggest that throughout the year, the hydrodynamic regime and physical forces will vary greatly, altering the rates and dynamics of sediment erosion and deposition.

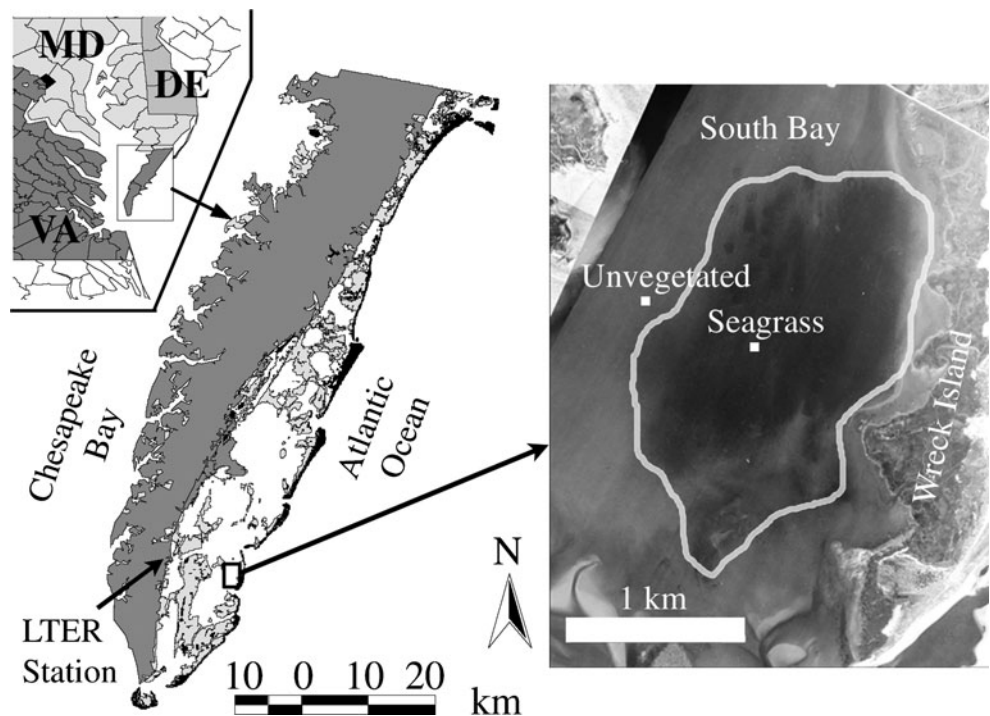
Though flow dynamics in seagrass meadows have been investigated in a number of studies; to date, most research has focused on observations conducted during the summer under full-growth conditions, while few studies have considered how structural and morphological changes that occur in seagrasses throughout the seasons of the year impact flow and sediment suspension. In order to determine the effects of seasonal growth and senescence of a seagrass meadow on hydrodynamics and sediment suspension, a *Z. marina* meadow in South Bay, Virginia, was monitored in summer, fall, winter, and spring conditions from June 2010 to June 2011 and compared to flow and sediment dynamics occurring at an adjacent, primarily unvegetated region. The goals of this study were to quantify the (1) seasonal variability of *Z. marina* morphology within a coastal bay, (2) flow and turbulence structure within and above the seagrass meadow due to the combined influence of waves and tidally driven flows, and (3) response of suspended sediment concentrations to variations in the magnitude of bed shear stresses.

Methods

Study Area

Field studies were performed within a *Z. marina* seagrass (eelgrass) meadow in South Bay, Virginia, USA (Fig. 1); a coastal bay within the Virginia Coast Reserve (VCR) where ongoing seagrass restoration efforts are being performed (Orth and McGlathery 2012). The VCR is characterized by contiguous marsh, shallow coastal bay, and barrier island systems and is a National Science Foundation Long-Term Ecological Research site. South Bay lacks any significant riverine discharge, and therefore turbidity is primarily controlled by local resuspension. The shallow depth of South Bay, typically <2 m, makes the bed sediments

Fig. 1 Delmarva Peninsula, USA showing the landmass, barrier islands (gray), and coastal bays. Labeled points represent the Long-Term Ecological Research (LTER) station where wind data were gathered, the unvegetated reference site (unvegetated), and the seagrass site (seagrass) within the large *Z. marina* meadow in South Bay, Virginia



susceptible to suspension from both wind waves and tidal currents (Hansen and Reidenbach 2012). In addition, low pelagic primary productivity in the coastal bays suggests that non-algal particulate matter primarily controls light attenuation (McGlathery et al. 2001).

A high-density seagrass site and an adjacent unvegetated reference site within South Bay were examined in June 2010 (summer), October 2010 (fall), January 2011 (winter), March 2011 (spring), and June 2011 (summer). Mean air temperature during sampling within each season was 21, 20, 0, 7, and 24 °C, respectively. During June 2010, the total *Z. marina* cover in South Bay was estimated to be 1,020 ha (Orth et al. 2012). The unvegetated site, located adjacent to the meadow containing very few, small patches of seagrass, was monitored as a reference for flow characteristics in the absence of any considerable benthic vegetation.

During each season, seagrass shoot density was measured in the field, while blade length and the number of blades per shoot were measured in the lab from seagrass collected at each site (Table 1), and canopy height was calculated as the average of the longest 2/3 of the seagrass blade lengths (Koch et al. 2006). Blade width and the spacing between blades were obtained via image analysis in ImageJ from pictures captured during each season. In order to quantify the meadow structure, a metric was developed incorporating the blade area and meadow density. Following Nepf (2012), frontal area is defined as ah , where $a=d/\Delta S^2$, d is blade width, ΔS is the spacing between canopy elements (i.e., seagrass blades), and h is the canopy height. Values for each season are listed in Table 1.

Instrumentation

Two acoustic Doppler velocimeters (ADV, Nortek® Vector), coupled with optical backscatter sediment sensors (OBS, Campbell Scientific® OBS 3+), were placed at $z=0.5$ and 0.1 m above the seafloor at the seagrass and unvegetated sites to quantify velocity and suspended sediment concentrations for a 72-h period. Measurement heights were chosen to obtain fluid velocities and sediment concentrations both within and above the seagrass meadow. In order to prevent seagrass from interfering with the measurements, a 0.15-m diameter patch of grass was removed from below each sensor head. Velocities were measured at each site in 10-min bursts every 20 min at a sampling rate of 32 Hz. Instantaneous velocity measurements were collected in the east, north, and up reference frame using the internal compass and tilt sensors of the velocimeters, and then rotated for each burst interval to align the flow along the dominant flow direction, u , while minimizing flow in the transverse direction, v , and leaving the vertical direction, w , unchanged. Each ADV was equipped with a pressure sensor, which was used to determine the water depth and characterize the wave climate with parameters such as significant wave height (H_s), average wavelength (L), and wave period (T) using linear wave theory (Dean and Dalrymple 1991). To obtain general flow characteristics at each site, a high-resolution Nortek Aquadopp® acoustic Doppler current profiler (ADCP) measured water velocities in 3-cm bins, between 0.2 and 1.0 m above the bottom at a sampling rate of 1 Hz for 10-min bursts every 20 min. During each season,

Table 1 *Z. marina* seagrass morphometrics for South Bay, Virginia

	Blade length (cm)	<i>n</i>	Canopy height (cm)	<i>n</i>	Density (shoots m ⁻²)	<i>n</i>	Blade width (cm)	<i>n</i>	Blades/shoot	<i>n</i>	Frontal area
June 2010	21±8	158	25±5	105	560±70	9	0.3±0.1	19	4.8±1.3	33	2.9±1.3
October 2010	19±7	59	23±5	39	350±50	6	0.2±0.1	25	3.0±0.9	20	0.7±0.3
January 2011	13±7	52	16±5	34	310±60	4	0.2±0.1	20	2.6±1.0	20	0.3±0.1
March 2011	12±5	91	15±3	60	350±90	6	0.2±0.1	20	4.0±1.4	20	0.5±0.3
June 2011	23±11	93	29±8	62	440±140	10	0.2±0.1	82	4.2±1.2	22	1.3±0.9

n number of samples for each average

Values represent the mean and standard deviations. Canopy height represents the average of the longest 2/3 of the seagrass blades sampled and frontal area is calculated as ah , where $a=d/\Delta S^2$, d is blade width, ΔS is the spacing between canopy elements, and h is the canopy height

two ADVs along with two OBSs were placed within the seagrass meadow for 72 h, then moved to an adjacent unvegetated seafloor for 72 h. During instrument deployments within the seagrass meadow, an additional ADCP and OBS sediment sensor were simultaneously deployed at the unvegetated site to collect water velocities, water depth, and suspended sediment concentrations. Wind data were obtained from a meteorological station in Oyster, VA, USA located approximately 4 km from South Bay.

Calibrations to relate backscatter intensity obtained from the OBS to suspended sediment concentrations were performed using sediment collected from the seagrass meadow and unvegetated site (technique described in Hansen and Reidenbach 2012). Sediment grain size distributions were characterized using a laser diffraction particle size analyzer (Beckman Coulter LS 13 320). D_{84} , the grain size diameter for which 84 % of the sample grain diameters are smaller, at the unvegetated site was $157\pm 7\ \mu\text{m}$; while at the seagrass site, sediments were finer at $130\pm 17\ \mu\text{m}$.

Wave–Turbulence Decomposition

In flows with both currents and waves, the covariance in velocity associated with waves is often larger than that associated with turbulence, and a wave–turbulence decomposition must be performed. When waves and currents are present, the instantaneous horizontal and vertical velocities can be written as:

$$\begin{aligned} u &= u' + \tilde{u} + \bar{u} \\ w &= w' + \tilde{w} + \bar{w} \end{aligned} \quad (1)$$

where \bar{u} and \bar{w} are the horizontal and vertical components of the mean velocity, \tilde{u} and \tilde{w} are the wave-induced orbital velocities, and u' and w' are the turbulent velocities. Most methods of wave–turbulence decomposition rely on two or more spatially separated velocity sensors to decouple wave motion from that of turbulence (Trowbridge 1998), or use simultaneous free surface displacement and velocity measurements to estimate wave motion at depth (Benilov and

Filyushkin 1970). Although these methods work well over relatively smooth beds, neither technique can be applied where bed topography significantly alters oscillatory flow structure outside the relatively thin wave boundary layer. A method of wave–turbulence decomposition that can be employed within seagrass systems uses a spectral decomposition, known as the Phase method (Bricker and Monismith 2007), where the phase lag between the u and w components of the surface waves from one velocity sensor are used to interpolate the magnitude of turbulence under the wave peak. In this method, the turbulent Reynolds stress can be quantified as the difference between the total stress and the wave stress (Hansen and Reidenbach 2012):

$$\overline{u'w'} = \overline{uw} - \overline{u\tilde{w}} \quad (2)$$

Both the total stress and wave stress can be computed from the Fourier transforms of the individual velocity components, u and w . For example, the wave stress becomes:

$$\overline{u\tilde{w}} = \sum_{j=-N/2}^{j=N/2} \tilde{U}_j^* \tilde{W}_j \quad (3)$$

where $U_j = U(f_j)$ is the Fourier transform of $u(t)$ at the frequency f_j and $*$ denotes the complex conjugate of U_j , which is multiplied by \tilde{W}_j , the Fourier transform of $w(t)$ at the frequency f_j . Equation 3 assumes that waves and turbulence do not interact, and the magnitude of \tilde{U}_j is the difference between the raw U_j and the turbulence U'_j that is interpolated below the wave peak via a least squares fit straight line, as shown in Fig. 2. The same method was used to solve for \tilde{W}_j . Since waves dominate the spectra under the wave peak, this method also assumes that the phase difference between u and w is dominated by the wave flow. Estimates for \overline{uw} were computed in a similar manner as Eq. 3 by using the full spectrum U_j and W_j . Estimates of $\overline{u'w'}$ from the Phase method were compared to the Benilov and Filyushkin (1970) method outside regions impacted by the seagrass canopy and agree to within $\pm 10\%$ $\overline{u'w'}$.

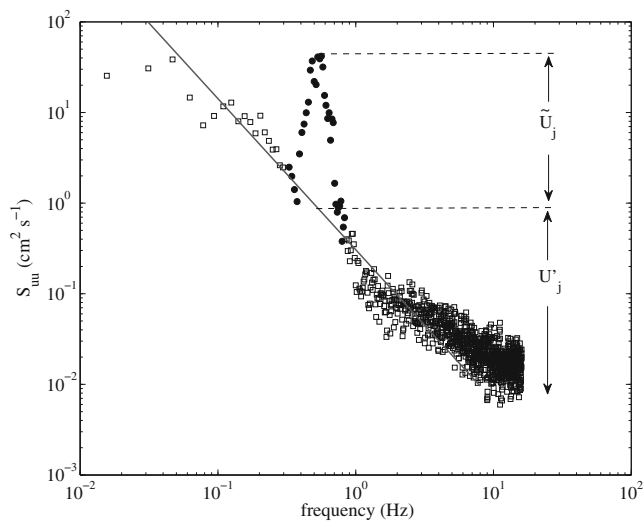


Fig. 2 Power spectral density (PSD) of the horizontal velocity, S_{uu} , for a 10-min representative data series computed at $z=0.5$ m at the seagrass site. The region encompassing the wave peak is denoted by the *solid circles*, while the *squares* represent the region of the spectra outside the wave domain. The *gray solid line* represents the least squares fit to the data outside the wave domain. The wave component of the stress, S_{uu} , is removed by subtracting the PSD formed above the *gray line* that encompasses the region of the wave peak

For time periods when waves were present, the horizontal wave orbital velocity, u_{os} , was calculated by summing the contributions from wave spectra across each frequency component of the horizontal and transverse velocity, u and v (Wiberg and Sherwood 2008). u_{os} is equivalent to the root mean squared orbital velocity and was computed both at $z=0.5$ and 0.1 m. Techniques for wave–turbulence decomposition and estimating u_{os} are described more fully in Hansen and Reidenbach (2012).

Bottom Shear Stress

The total bed shear stress, τ_b , was calculated as the square root of the sum of the squares of the bed stress due to waves, τ_{wave} , and currents, $\tau_{current}$ (Wiberg and Smith 1983), from wave orbital velocity and turbulent kinetic energy measured at $z=0.1$ m above the seafloor:

$$\tau_b = \sqrt{\tau_{wave}^2 + \tau_{current}^2} \tag{4}$$

Bottom shear stress due to waves was calculated from Fagherazzi and Wiberg (2009):

$$\tau_{wave} = \frac{1}{2} f_w \rho u_b^2 \quad f_w = 0.04 \left[\frac{u_b T}{2\pi k_b} \right]^{-0.25} \tag{5}$$

where f_w is the wave friction factor, k_b is the characteristic roughness length estimated as $3D_{84}$ (Lawson et al. 2007), and u_b is the bottom orbital velocity, which was approximated using estimates of u_{os} computed at $z=0.1$ m. The

current shear stress was estimated as (Stapleton and Huntley 1995; Widdows et al. 2008):

$$\tau_{current} = \rho u_{*current}^2 = 0.19 \rho (\text{TKE}) \tag{6}$$

where TKE is the turbulent kinetic energy calculated from the turbulent portion of the velocity spectrum:

$$\text{TKE} = 0.5 (\overline{u'^2} + \overline{v'^2} + \overline{w'^2}) \tag{7}$$

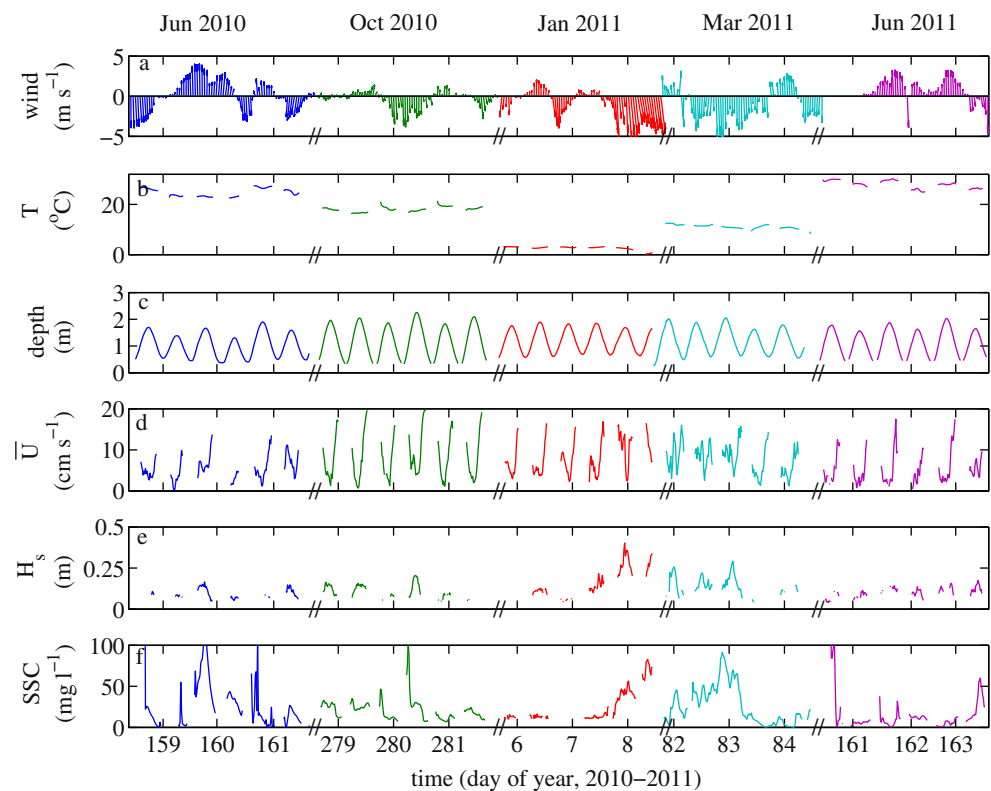
Values of TKE were used to estimate shear stress instead of Reynolds stress (where $\tau = -\rho \overline{u'w'}$, commonly called the covariance method) because the covariance method assumes a logarithmic velocity profile has formed within an equilibrium boundary layer, which is rarely observed within a seagrass canopy. Although waves can alter Reynolds stress and TKE in the presence of a mean current (Grant and Madsen 1979), previous findings within South Bay (Hansen and Reidenbach 2012) suggest only minor alteration in the magnitude of TKE in the presence of small-amplitude wind waves, and therefore Eq. 6 can be reasonably applied.

Results

Average blade length and canopy height for each season are listed in Table 1, and were statistically greater in the summer (June) and fall (October) than in January and March (one-way ANOVA with Bonferroni multicomparison, $p < 0.05$). Both the shoot density (shoots per square meter) and blades per shoot were statistically lower in winter than summer, creating a more patch-like distribution (one-way ANOVA with Bonferroni multicomparison, $p < 0.05$). The blade frontal area decreased from a maximum value of 2.9 ± 1.3 during June 2010 to a minimum value of 0.3 ± 0.1 in January 2011.

Physical characteristics at the seagrass site for each season are shown in Fig. 3. Hourly wind speeds ranged between 0.1 and 8.2 m s^{-1} , while wind speeds averaged over the 3-day deployments varied from 1.7 to 3.3 m s^{-1} between seasons (Fig. 4). The unvegetated site was 0.8 km to the northwest of the seagrass site, and fetch distances from each site to surrounding barriers were mapped at 30° intervals. Wind directions were variable between seasons, and depending upon wind direction, fetch length ranged from 1 to 15 km at the seagrass site and 0.9 to 16 km at the unvegetated site. The range of fetch lengths was not significantly different between sites (one-way ANOVA, $p > 0.6$). Water temperature throughout the year ranged from 2.6 °C during January 2011 to 28.1 °C during June 2011. Dominant tidal flow was along a northeast/southwest direction at both the seagrass site and adjacent unvegetated site for all seasons. Mean depth at the seagrass site was 1.1 m and at the

Fig. 3 **a** Wind speed, *arrows* denote the direction toward which the wind is blowing, with northward up and eastward to the right; **b** water temperature; **c** water depth at the seagrass site; **d** root mean square horizontal water velocities averaged over 10-min burst intervals at $z=0.5$ m above the seafloor at the seagrass site **e** significant wave height (H_s) over the seagrass meadow, and **f** near-bed suspended sediment concentrations (SSC) within the seagrass meadow at $z=0.1$ m. Breaks in data represent periods when the instrument was out of the water, or in **e** when waves were not present



unvegetated site was 1.4 m, while tidal amplitude ranged from 0.5 to 0.8 m (Table 2). Significant wave heights at the unvegetated site ranged on average from 0.13 ± 0.05 to 0.21 ± 0.07 m throughout the year. At the seagrass site, significant wave heights ranged from 0.10 ± 0.03 m during June to 0.18 ± 0.09 m during January.

Seasonal variations in mean velocities above ($z=0.5$ m) and within ($z=0.1$ m) the seagrass canopy and adjacent

unvegetated reference site ($z=0.5$ m) are shown in Fig. 5a. Mean velocities at the unvegetated site did not vary significantly at $z=0.5$ m between seasons (one-way ANOVA, $p=0.18$). Within the seagrass meadow, velocities were significantly smaller during the summer (June 2010, 2011) than at any other time of year (one-way ANOVA with Bonferroni multicomparison, $p<0.05$). In addition, there was a significant difference between the velocities measured at the seagrass and unvegetated sites during every season (one-way ANOVA with Bonferroni multicomparison, $p<0.05$), with the greatest reduction in flow between the two sites occurring during the summer (55–60 % at $z=0.5$ m) and least reduction during winter (40 % at $z=0.5$ m). Figure 5b shows that as frontal area increases, so does the percent velocity reduction within the canopy (at $z=0.1$ m) compared to above (at $z=0.5$ m). Average velocity reduction across all seasons between $z=0.1$ and 0.5 m at the unvegetated site was 44 %. At the unvegetated site, a logarithmic flow profile developed throughout the entire bottom boundary layer. However, at the seagrass site, greater attenuation of velocity occurred adjacent to the seafloor due to flow interaction with the meadow, creating an inflection point in the velocity profile at the top of the seagrass canopy (Fig. 6), which was strongest during summer.

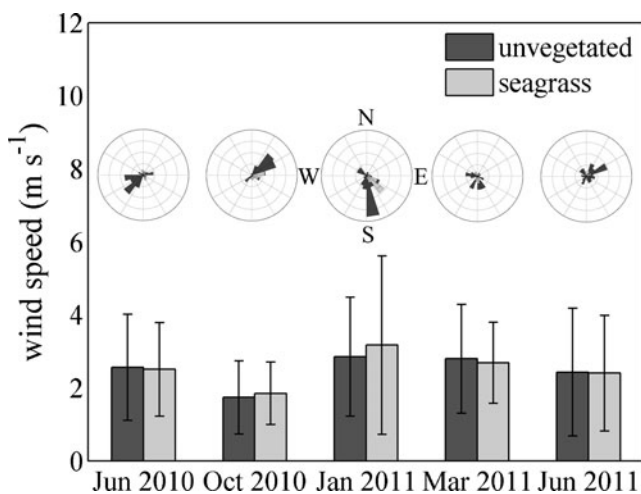


Fig. 4 Average wind speed (± 1 SD) and direction at both the unvegetated and seagrass sites for each season. Compass plots are histograms of wind direction with concentric rings each representing 20 vector samples and chords at 30° intervals

Waves and Orbital Motion

Waves in South Bay were locally developed wind waves with average wave periods (T) ranging from 1.4 to 1.9 s.

Table 2 Temporal averages of suspended sediment concentration (SSC), ± 1 SE, water depth, and tidal amplitudes (± 1 SD) during seasonal deployments at both an unvegetated reference site and over the seagrass meadow

	Seagrass SSC (mg l^{-1}) $z=0.5$ m	Seagrass SSC (mg l^{-1}) $z=0.1$ m	Unvegetated SSC (mg l^{-1}) $z=0.1$ m	Seagrass Depth (m)	Seagrass Tidal Amplitude (m)	Unvegetated Depth (m)	Unvegetated Tidal Amplitude (m)
June 2010	33 \pm 3	26 \pm 2	57 \pm 3	0.99 \pm 0.43	0.57 \pm 0.11	1.49 \pm 0.55	0.73 \pm 0.12
October 2010	16 \pm 1	19 \pm 1	15 \pm 2	1.04 \pm 0.59	0.83 \pm 0.08	1.44 \pm 0.49	0.62 \pm 0.11
January 2011	21 \pm 2	33 \pm 3	17 \pm 1	1.07 \pm 0.42	0.59 \pm 0.04	1.38 \pm 0.57	0.81 \pm 0.05
March 2011	23 \pm 2	27 \pm 2	25 \pm 2	1.15 \pm 0.49	0.65 \pm 0.09	1.27 \pm 0.41	0.52 \pm 0.03
June 2011	21 \pm 2	17 \pm 2	50 \pm 1	1.04 \pm 0.49	0.67 \pm 0.09	1.50 \pm 0.51	0.68 \pm 0.06

Significant wave heights (H_s) ranged from 0.10 to 0.21 m during sampling at both sites, but were smaller over the seagrass meadow than the unvegetated seafloor for all seasons except winter, even though wind speeds were

statistically similar within each season (Fig. 7, one-way ANOVA, $p > 0.08$). In addition, the reduction of H_s and T in the seagrass meadow scaled with increased seagrass canopy area, where the largest difference in H_s and T between the seagrass meadow and unvegetated site occurred during the summer. Wave development depends not only on frictional interaction with benthic vegetation, but also on wind speed and water column depth. Significant wave height and period plotted against wind speed (Fig. 8a,b) show that waves were larger and had longer periods over the unvegetated seafloor than over the seagrass meadow for any given wind speed except for weak wind conditions ($\leq 2 \text{ m s}^{-1}$) where there was no statistical difference in H_s (one-way ANOVA, $p > 0.05$). Additionally, both significant wave height and wave period were lowest for the fully developed meadow in the summer for all wind speeds. Wave height and period also increased with increasing water depth, but for any given water depth, waves were larger and had longer periods at the unvegetated site than compared to the seagrass site for all seasons of the year (Fig. 8c,d) except

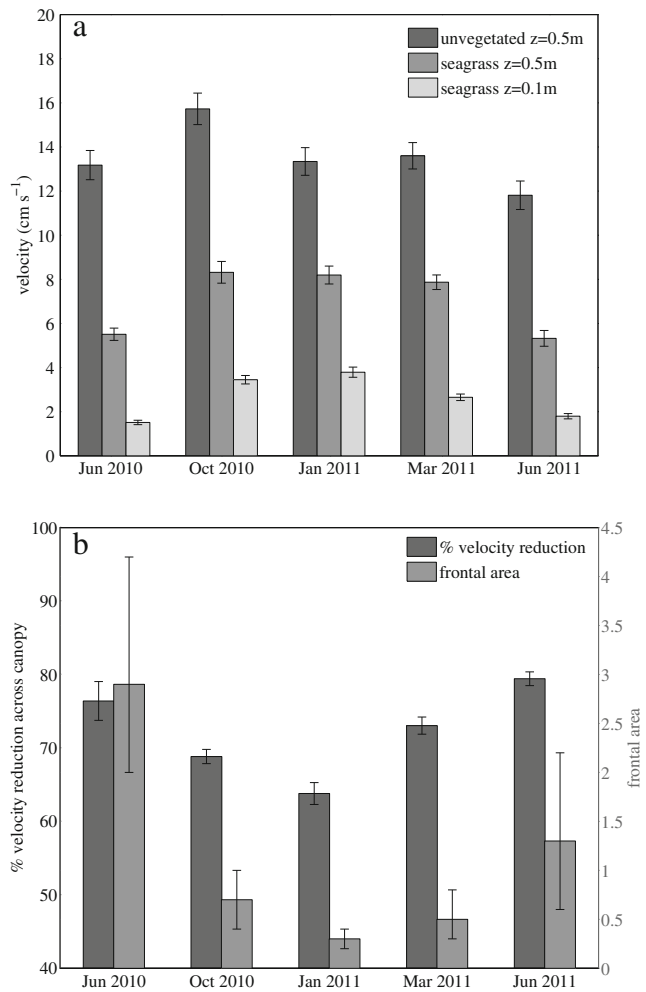


Fig. 5 **a** Average velocities (± 1 SE) at $z=0.5$ m above the seafloor at the unvegetated reference site, at $z=0.5$ and 0.1 m at the seagrass site, measured simultaneously. **b** Percent velocity reduction (± 1 SE) within the seagrass canopy (at $z=0.1$ m) compared to above the canopy (at $z=0.5$ m). Secondary y -axis represents the seagrass canopy frontal area per unit area of seafloor (± 1 SD)

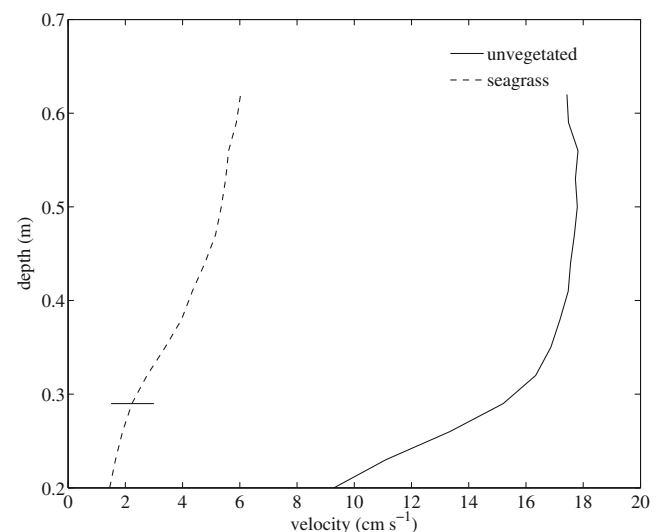


Fig. 6 Vertical profiles of horizontal velocity averaged over a single ebbing tide at the unvegetated and seagrass sites during simultaneous deployments in June 2011. Horizontal line represents the canopy height

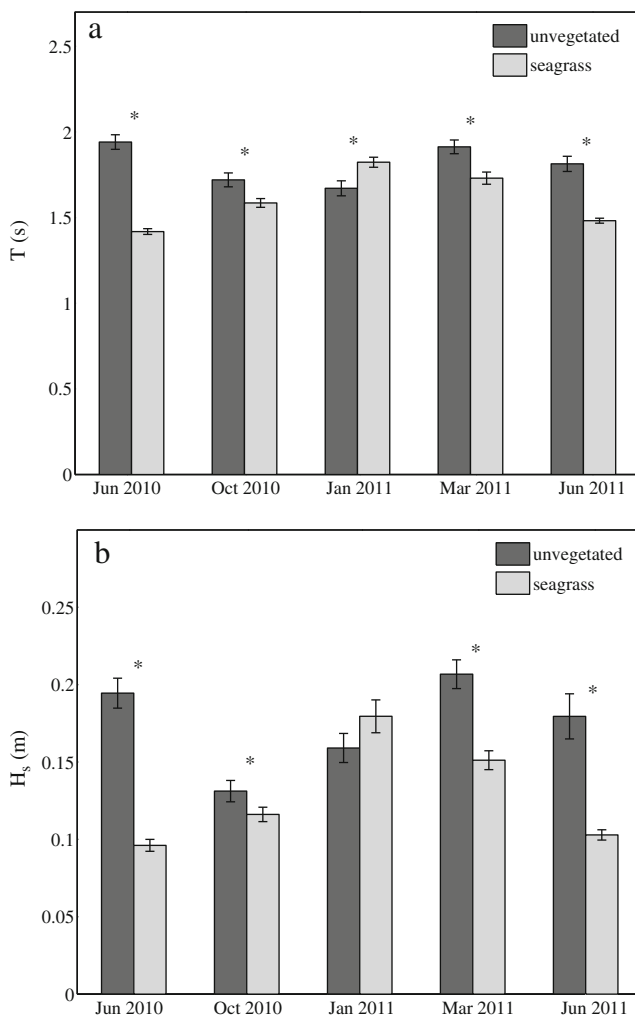


Fig. 7 **a** Significant wave period, T , and **b** significant wave height, H_s , for each season calculated from linear wave theory (± 1 SE). Asterisks above graphs indicate values are statistically different between the unvegetated and seagrass sites within the season

for January. In general, wave dynamics within the seagrass canopy matched the unvegetated site most closely during January, when seagrass cover was minimal.

Horizontal orbital velocities (u_{os}) above and within the meadow were computed using spectra of the horizontal wave motions. As expected, during all seasons orbital motions were greater at $z=0.5$ m than at $z=0.1$ m due to natural attenuation of short-period waves with depth (Fig. 9). Orbital motions were highest within the seagrass meadow in January and March when larger waves were able to develop due to the low percent cover of the seagrass. In January, the absence of seagrass cover also allowed longer period waves to develop (shown in Fig. 7a). In summer (June 2010 and June 2011), wave periods and orbital velocities were decreased, suggesting that the significant seagrass structure attenuated wave development over the meadow.

To determine the extent to which reduction of wave orbital velocities within the seagrass canopy was due to natural

attenuation with depth or interaction with the seagrass blades, orbital velocities (u_{os}) computed through velocity spectra were compared with estimates of wave orbital velocities (u_{om}) using pressure sensor measurements from the ADV. From linear wave theory for small amplitude, monochromatic waves, the horizontal component of orbital velocity, u_{om} , was computed as (Dean and Dalrymple 1991):

$$u_{om} = \frac{\pi H_s \cosh(kz)}{T \sinh(kh)} \quad (8)$$

where H_s is the significant wave height, k is the wave number such that $k=2\pi/L$ where L is the wavelength, T is wave period, z is the location above the seafloor, and h is the water column depth. The wavelength, L , was calculated according to linear

wave theory for intermediate waves as: $L = L_\infty \sqrt{\tanh\left(\frac{2\pi h}{L_\infty}\right)}$, where $L_\infty = \frac{g}{2\pi} T^2$.

Linear wave theory assumes the bed is frictionless and therefore, estimating wave orbital velocity decay with depth using linear wave theory (Eq. 8) and comparing it to computed orbital velocities using local velocity measurements within the canopy (u_{os}) should indicate the relative dampening of wave orbital velocity due to frictional interaction with the seagrass canopy. At the seagrass site, the orbital motion predicted by linear wave theory at $z=0.1$ m within the seagrass canopy was not significantly greater than that quantified through velocity spectra during any season of the year (one-way ANOVA, $p>0.05$), suggesting that the seagrass did not have a significant impact on the attenuation of wave orbital motion with depth (Fig. 9). This suggests that although seagrass attenuates the amplitude of waves as they propagate across the meadow, orbital motions are not attenuated due to direct interaction with the seagrass blades within the canopy.

The power spectral density (PSD) of horizontal velocities, S_{uu} , was examined to quantify the relationship between meadow structure, wave period, and turbulence intensity (Fig. 10). The velocity time series from each season was first filtered to select for wave-influenced periods, where the wave portion of the PSD accounted for greater than 10 % of the total energy. The frequency spectrum was then averaged over the remaining time series to obtain the average frequency distribution in each season. Figure 10a shows spectra comparing the unvegetated and seagrass sites in June 2011 while Fig. 10b shows spectra for January 2011. Although velocity measurements were not measured simultaneously within the seagrass and unvegetated sites, winds were comparable within each season, and therefore, wave statistics can be generally compared. The reduced magnitudes of S_{uu} within the seagrass meadow were indicative of lower turbulent energy compared to the unvegetated site, with greater reductions in S_{uu} occurring in the summer. Peaks in the spectra that

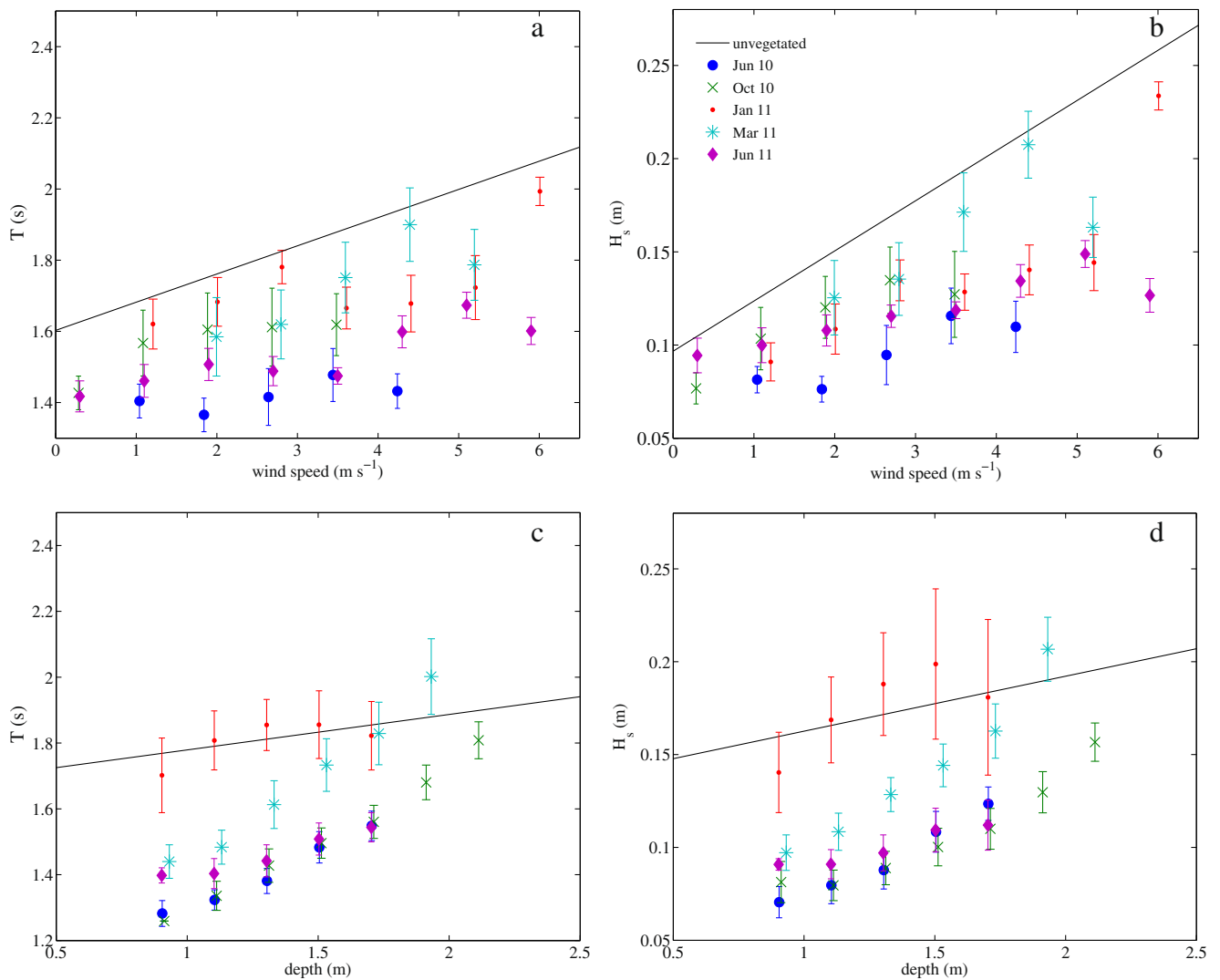


Fig. 8 **a** Average wave period, T , and **b** significant wave height, H_s , plotted as a function of wind speed (± 1 SE). **c** Average wave period, T , and **d** significant wave height, H_s , plotted as a function of water depth (± 1 SE). Data collected at the seagrass site during each season were

averaged using a running mean with a 0.8 m s^{-1} averaging window for wind speed and 0.2 m for water depth. *Solid black line* represents best-fit line for all seasons at the unvegetated site

occur between $f=0.2$ and 1 Hz were due to orbital wave motion and indicated that wave energy was reduced within the meadow during June compared to the unvegetated site (one-way ANOVA, $p<0.05$), but was not significantly reduced during January (one-way ANOVA, $p=0.98$). In addition, wave motion at low frequencies was reduced within the seagrass meadow in June ($0.3<f<0.6 \text{ Hz}$) compared to the unvegetated site, but was not substantially altered during January; all suggesting that under high seagrass meadow development, both wave heights and wave periods were reduced.

Turbulence and Momentum Transport

After removal of orbital motions due to waves, Reynolds stresses were calculated from the turbulence portion of the

velocity spectrum at $z=0.5$ and 0.1 m within the seagrass meadow (Fig. 11). Reynolds stress was then normalized by ΔU^2 , which is defined as the difference between velocities measured at $z=0.5$ and 0.1 m ($\Delta U=U_{0.5 \text{ m}}-U_{0.1 \text{ m}}$). The greatest reduction of within-canopy Reynolds stress occurred in June, when the canopy frontal area was greatest. In October, during initial senescence of the meadow, turbulence levels increased within the canopy, and in January and March, when the meadow frontal area was minimal, enhanced turbulence within the canopy was measured relative to above (at $z=0.5 \text{ m}$). Compared to the unvegetated site, the most dramatic reductions of within-canopy Reynolds stress occurred in summer, with enhanced Reynolds stresses in winter. The absolute magnitude of Reynolds stress followed these same normalized trends throughout the seasons at both the unvegetated and seagrass sites.

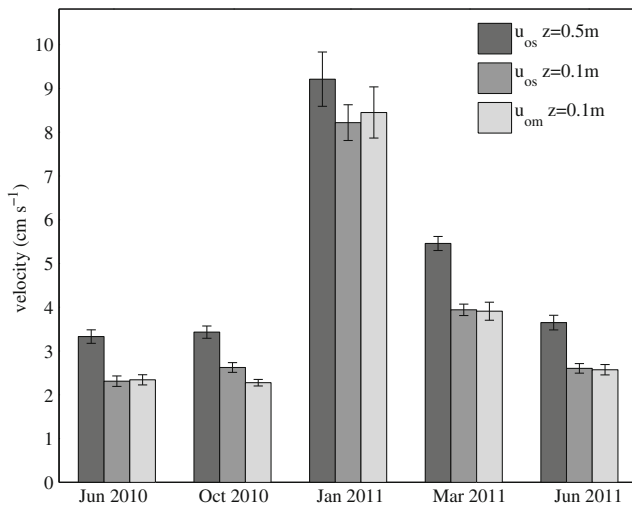


Fig. 9 Horizontal orbital velocities, u_{os} , above ($z=0.5$ m) and within ($z=0.1$ m) seagrass meadows from spectral analysis, as well as expected orbital velocities, u_{om} , calculated via linear wave theory. Linear wave theory predictions were never significantly greater than horizontal orbital velocities measured from spectral analysis (one-way ANOVA, $p<0.05$). Error bars ± 1 SE

To determine how turbulent fluctuations contribute to the transport of momentum throughout the bottom boundary layer, quadrant analysis was performed. Velocity fluctuations, u' and w' , were normalized by their respective standard deviations and divided into four quadrants based on the sign of their instantaneous values (Lu and Willmarth 1973). The two dominant quadrants responsible for momentum transfer are quadrant 2 (Q2), where turbulent ejections of low momentum fluid are transported vertically upward ($u'<0$, $w'>0$), and quadrant 4 (Q4), where sweeping events transport high momentum fluid downward towards the seafloor ($u'>0$, $w'<0$). These ejections and sweeps lead to periodic mixing across the seagrass canopy–water interface. Contours of the turbulent probability distribution function are shown in Fig. 12 for turbulent motions at $z=0.1$ m at the unvegetated and seagrass sites in June 2011 during periods with no wave action (i.e., energy within the wave portion of the PSD accounted for less than 10 % of the total energy). At the unvegetated site, the distribution of momentum was balanced between Q2 and Q4 with Q1 (16 %), Q2 (33 %), Q3 (16 %), and Q4 (35 %). In comparison, at the seagrass site, the distribution was Q1 (11 %), Q2 (26 %), Q3 (10 %), and Q4 (53 %). These sweeping events transport high momentum fluid down into the meadow from the overlying water. The combined Q2 and Q4 contributions accounted for 79 % of the total Reynolds stress in the seagrass canopy, compared to 68 % at the unvegetated site. This indicates that though Reynolds stress was smaller within the seagrass canopy, turbulent motions were more efficient in the vertical transport of momentum compared to the unvegetated site. The increasing shift toward motion in Q2 and Q4 also correlated with increasing canopy frontal area. In January and March,

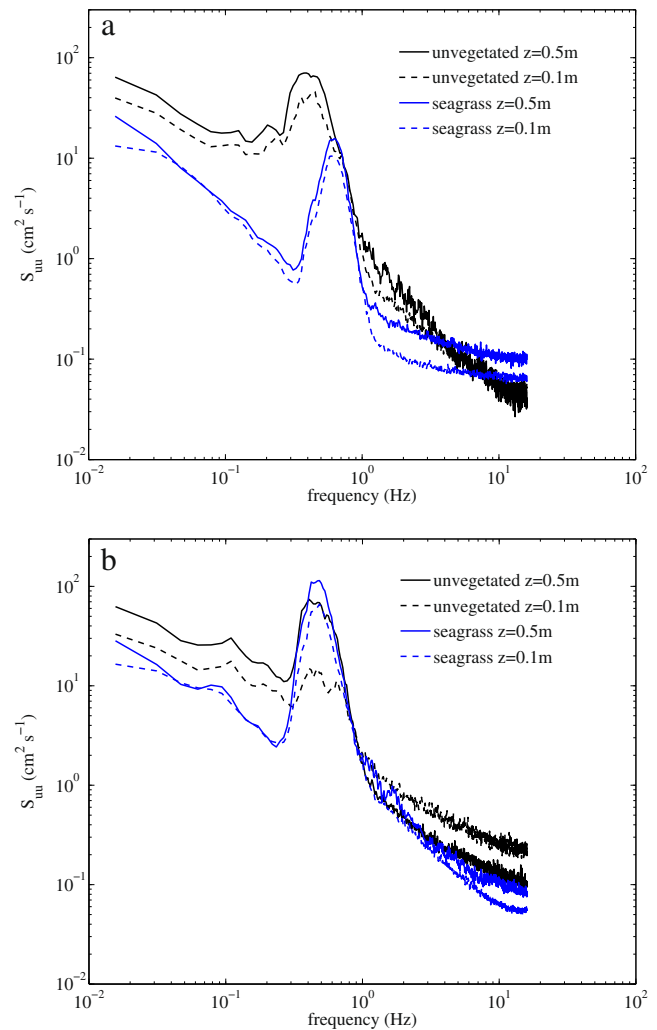


Fig. 10 Power spectral density (PSD), S_{uu} , for periods with wave activity for **a** June 2011 and **b** January 2011. Spectra were formed by averaging individual spectra, of length $n=2048$ velocity records, over time periods when the wave portion of the PSD accounted for greater than 10 % of the total energy of the flow. Peaks in the PSD between frequencies (f) of $0.2 \leq f \leq 1$ Hz represent water motion due to waves. Flattening of the spectra at high frequencies ($f > 5$ – 10 Hz) represents the noise floor of the instrument

combined Q2 and Q4 shifts are 74 and 73 %, respectively, at $z=0.1$ m. With increased seagrass canopy development in the summer, contributions to Q2 and Q4 increased to 87 and 79 % during June 2010 and 2011.

Bottom Shear Stress and Suspended Sediment Dynamics

The total stress imparted to the seafloor was quantified using a combined bottom shear stress, τ_b (Eq. 4), calculated as the square root of the sum of the squares of the shear stress due to waves, τ_{wave} (Eq. 5), and due to currents, $\tau_{current}$ (Eq. 6; Wiberg and Smith 1983). Over the unvegetated seafloor, shear stress was consistently greater than that produced

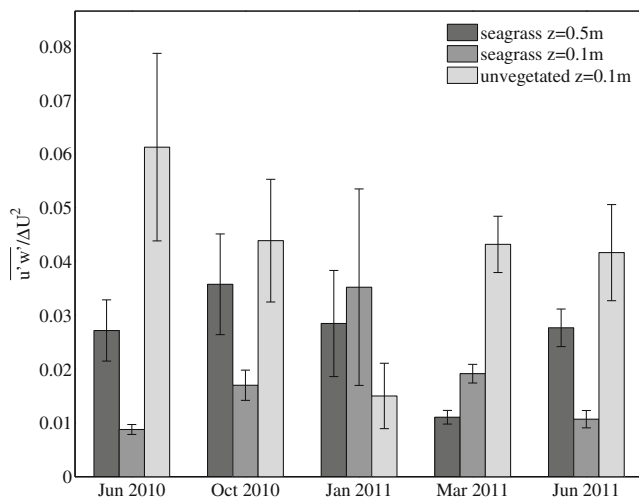


Fig. 11 Reynolds stress for turbulence portion of velocity spectrum above ($z=0.5$ m) and within ($z=0.1$ m) the seagrass meadow and at the unvegetated site ($z=0.1$ m). Reynolds stress is normalized by ΔU^2 , which is defined as the difference between mean velocities measured at $z=0.5$ m and 0.1 m, $\Delta U=U_{0.5\text{ m}}-U_{0.1\text{ m}}$. Error bars ± 1 SE

within the seagrass meadow (Fig. 13a). At the seagrass site, τ_b was largest during January (Fig. 13b) and lowest in the summer.

Although the critical shear stress that can initiate sediment resuspension was not directly quantified in South Bay, estimates within Hog Island Bay, which is directly adjacent to South Bay in the VCR, were performed by Lawson et al. (2007) and found to be $\tau_{cr}=0.04\text{ N m}^{-2}$ over unvegetated sites adjacent to seagrass meadows. This value is in agreement with $\tau_{cr}=0.05\text{ N m}^{-2}$ found by Widdows et al. (2008) for unvegetated seafloor sediments in the North Sea, where adjacent *Z. marina* meadows had a $\tau_{cr}=0.07\text{ N m}^{-2}$. Increased abundances of microphytobenthos and lower densities of grazers were found to be the cause for increased sediment stabilization within the *Z. marina* meadow. This suggests that $\tau_{cr}=0.04\text{ N m}^{-2}$ is likely a reasonable estimate for unvegetated regions and a conservative estimate for the eelgrass meadow in South Bay. To determine the influence of the meadow on sediment suspension, shear events with magnitudes greater than this critical shear stress necessary for sediment suspension were isolated. At the unvegetated site, greater than 90 % of the deployment times had bed shear that was sufficient for initiating sediment suspension. Within the seagrass meadow, bed shear was greater than critical shear stress for 55 % of the deployment time period in the summer and fall, while winter and spring had bed shear stresses that exceeded the critical stress threshold 80–85 % of the time. Corresponding reductions in suspended sediment concentrations (SSC) at the seagrass site, as compared to the unvegetated site, were highest during the summer (60 % reduction). During the spring, the magnitude of SSC within the canopy was not significantly different than that near the seafloor at the

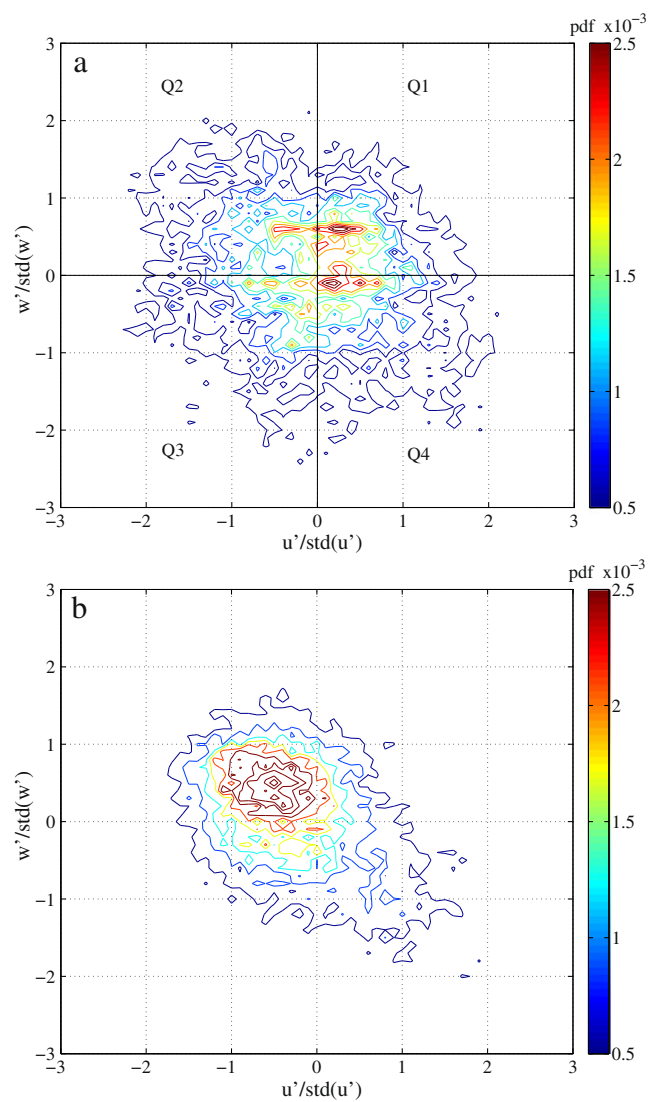


Fig. 12 Quadrant analysis of the probability density functions (pdfs) of u' and w' distributions normalized by their standard deviation at **a** $z=0.1$ m above the seafloor at the unvegetated site and **b** $z=0.1$ m at the seagrass site, which shows the dominance of turbulent sweeping events in quadrant 4

unvegetated site (at $z=0.1$ m, one-way ANOVA, $p>0.48$). Interestingly, in winter, SSC was significantly enhanced, up to two times (one-way ANOVA, $p<0.05$) in the seagrass meadow compared to the adjacent unvegetated site (Table 2).

A two-dimensional PSD of horizontal velocities is shown for the seagrass site in Fig. 14a for frequencies between 0 and 2 Hz. This plot includes the tidally-dominated contributions to the spectra at small frequencies (i.e., $f<0.3$ Hz), as well as the wave component of the PSD, which typically span the range $0.3<f<1$ Hz. Peak wave frequency at high tide was approximately $f=0.5$ Hz ($T=2$ s), but as the water depth decreased, peak wave frequency increased to approximately $f=1$ Hz, indicating a reduction in the peak

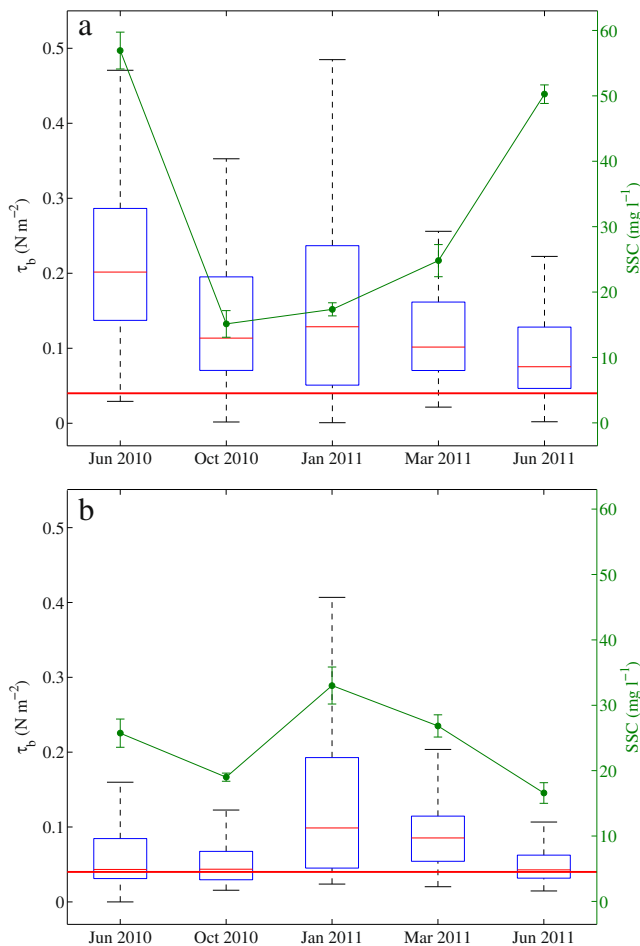


Fig. 13 Bed shear stress, τ_b , at the **a** unvegetated site and **b** seagrass meadow. Horizontal line within the box indicates median τ_b , while the lower and upper edges of the box represent the 25th and 75th percentiles, respectively. Whiskers extending from the box indicate the minimum and maximum measured τ_b . Horizontal red line across both plots represents the critical stress threshold for the suspension of sediment. Average suspended sediment concentrations (± 1 SE) measured at $z=0.1$ m above the seafloor are plotted in green with the secondary y-axis

wave period to $T=1$ s. Time periods with highest wave energy (i.e., high PSD in the wave band $0.3 < f < 1$ Hz), corresponded closely to time periods with enhanced SSC (Fig. 14b). A Pearson linear correlation factor, defined as the covariance of two variables divided by the product of their standard deviations, was computed to determine the relationship between suspended sediment and orbital motion near the seafloor. At the seagrass site, SSC values near the seafloor ($z=0.1$ m) were positively correlated with wave orbital velocities in all seasons, with correlation factors ranging from 0.47 to 0.67 ($p < 0.05$). However, enhanced SSC values were not significantly correlated to enhanced mean currents, indicating waves were the dominant mechanism initiating sediment resuspension.

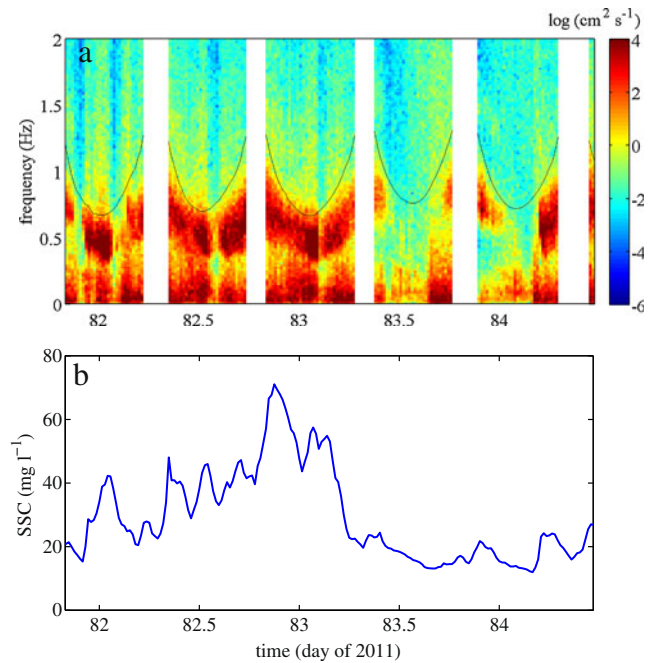


Fig. 14 **a** Two-dimensional power spectral density of horizontal velocities at $z=0.1$ m above the seafloor at the seagrass site during March 2011. Black lines indicate $f = \sqrt{g/[4\pi(h-z)]}$, the frequency (f) at and above which linear wave theory predicts wave motion is attenuated due to water depth. Regions with no data were during low tide when the velocimeter had poor signal quality. **b** Corresponding SSC at $z=0.1$ m, indicating correlation between periods of high wave activity and increased SSC

Discussion

Z. marina meadows within a Virginia coastal bay were found to substantially lower overall mean currents compared to an adjacent unvegetated site's flow conditions during all seasons of the year. Average velocities were 1.6–2.4 times lower at the seagrass site than at the unvegetated site even though tidal amplitude was statistically similar (average tidal amplitude during deployments at the seagrass site was 0.67 ± 0.10 m and at the unvegetated site was 0.67 ± 0.11 m; Table 2).

Near-bed flows within the seagrass meadow were dramatically reduced, but varied seasonally in response to seagrass canopy area as expected. Yearly averaged, mean velocity at $z=0.1$ m at the unvegetated site was 9.2 cm s^{-1} , while mean flow at the seagrass site was 2.6 cm s^{-1} . The greatest flow reduction within the canopy compared to above occurred during June, while the smallest within-canopy flow reduction occurred in January. This agrees with predicted shear layer development, where shear layers are expected to form when $ah > 0.1$ (Nepf 2012). In shear layers, velocity profiles above the meadow become logarithmic (Kaimal and Finnigan 1994), while velocities rapidly decrease within the canopy, creating an inflection point near

the canopy–water interface. Due to seasonal changes in seagrass cover, altering both the canopy height and canopy frontal area, the precise location of an inflection point could not always be determined. However, $ah > 0.1$ occurs during all seasons of the year, while $ah > 1$ in the summer. For sparse canopies, a coherent canopy shear layer is not formed, rather, characteristics of both shear layer and rough-wall boundary layers are present, with reduced shear layer development occurring as flow velocity increases (Lacy and Wyllie-Echeverria 2011). When $ah > 1$, the canopies become essentially cutoff from overlying flow (Luhar et al. 2008), dramatically reducing within-canopy velocities.

Tidally- and wave-dominated flows were separated using the magnitude of power density within the wave band of the frequency spectra. In the fully developed canopy in the summer, normalized Reynolds stress within the canopy was reduced by 75–85 % compared to measurements at the same elevation of $z=0.1$ m at the unvegetated site. The highest turbulence levels within the seagrass meadow were found at the lowest seagrass canopy frontal area, and Reynolds stress was greater within the canopy than above in the winter and spring. Turbulence enhancement can be caused both by reduced stem density that can increase stem-generated wake turbulence (Nepf et al. 1997; Widdows et al. 2008), or by a reduction in meadow height, causing an intensification of turbulence closer to the seafloor from the fluid shear layer formed at the top of the canopy (Abdelrhman 2003; Gambi et al. 1990). Additionally, in sparse canopies, significant turbulence can be generated by flow interaction with the seafloor (Lacy and Wyllie-Echeverria 2011). Both blade length and density contribute to changes in frontal area. Luhar et al. (2008) found that when frontal area is substantially greater than ~ 0.1 , the canopy acts as a dense canopy. In dense canopies, within-canopy turbulence and flow are significantly reduced and roughness length-scales decrease with increasing frontal area due to the mutual sheltering of individual canopy elements (Luhar et al. 2008). When the frontal area reaches approximately ≥ 1 , flow is almost entirely displaced above the canopy, substantially limiting turbulence that can contribute to sediment resuspension (Luhar et al. 2008). Luhar et al. (2008) also noted that by reducing the momentum penetration, a dense canopy shelters itself from high flow, which is critical during extreme events such as floods, and the reduction in bottom stress associated with dense canopies can stabilize the bed and improve water clarity. Our results indicate that under summer conditions, the Virginia seagrass meadow was acting as a dense canopy (frontal area of 1.3–2.9), which both reduced bottom stress and stabilized sediments compared to the unvegetated seafloor. Although there is a transition region for canopies with frontal areas between 0.1 and 0.5, Luhar et al. (2008) found when frontal area is less than ~ 0.1 , the canopy acts as a sparse canopy. In sparse canopies, the flow penetrates throughout the entire canopy and turbulence intensities

increase with frontal area, as stem–wake flow interactions are enhanced (Raupach et al. 1996). Our results in winter (frontal area of 0.3 ± 0.1 , within the transitional region) agree with conditions found for a sparse canopy, which include flow penetration through the canopy and increased turbulence intensities contributing to enhanced bottom shear stress and sediment suspension compared to the unvegetated site.

Quadrant analysis indicated that during all seasons, turbulent motion within the meadow was dominated by sweeping events of momentum, suggesting turbulence was generated at the shear layer at the top of the canopy and momentum transport occurred into the canopy. Although the magnitude of turbulence within the canopy was reduced with increased seagrass coverage, the efficiency of momentum transport increased, as evident from the greater relative contributions from both ejection and sweep motions of turbulent eddies transporting momentum into the canopy. Strong sweep motions into the canopy were also observed by Ghisalberti and Nepf (2006), who found that sweeps were followed by weak ejection events ($u' < 0$, $w' > 0$) that occurred at frequencies twice that of the dominant frequency of the coherent vortex formed at the top of the canopy.

Wave Interaction with the Seagrass Canopy

Wave periods and significant wave heights were computed from pressure records obtained from the ADVs at a sampling rate of 32 Hz. Wave periods at all sites ranged between 1 and 4 s, representing wind generated gravity waves. Over the year, there was a 35 % reduction in H_s at the seagrass site compared to the unvegetated site. Most of this reduction occurred during the summer, with no statistical difference in H_s during the winter. As evident from PSD graphs (Fig. 10), waves were not monochromatic and typically spanned a range of frequencies between $f=0.3$ to 1 Hz. When comparing attenuation of wave energy within this wave portion of the PSD, the largest reductions in wave motion within the seagrass bed compared to the unvegetated site occurred at low frequencies during the summer. Bradley and Houser (2009) found that waves at $T \sim 2.6$ s were relatively unaffected by seagrass, but higher frequency waves ($T \sim 1.5$ s) caused seagrass blade movement that tended to be out of phase with wave motion, increasing frictional drag and wave energy attenuation. Waves in our study tended to be of shorter period, and most of the attenuation in wave energy occurred between wave periods of $T=1.4$ – 2.0 s. Although blade movement was not quantified in our study, this attenuation is within the same frequency range as that found by Bradley and Houser (2009).

The ratio of wave orbital excursion length (A) to blade spacing (ΔS) can also be used to indicate the significance of wave orbital motion reduction within the canopy (Lowe et al. 2005). As per Lowe et al. (2005), $A = u_{os}/\omega$, where u_{os} is

the wave orbital velocity and $\omega=2\pi/T$, is the radian wave frequency estimated directly above the canopy at $z=0.5$ m. For $A/\Delta S > 1$, the attenuation of orbital motion within the canopy is significant. Our measurements show that $A/\Delta S$ ranged between 0.5 during summer and 0.75 during winter. This indicates that orbital motions are not significantly altered due to direct interaction with the seagrass blades, and although tidally driven flows may be damped, oscillatory motion was able to effectively penetrate the seagrass canopy. This finding is similar to laboratory measurements of flow structure within and above a model *Z. marina* meadow (Luhar et al. 2010), which found that although unidirectional flows were reduced within the meadow, in-canopy orbital velocities were not significantly altered. This suggests that throughout the year, storm events, which tend to increase H_s and T (Chen et al. 2005), may be effective at generating oscillatory flows through the seagrass canopy. However, since attenuation in wave amplitudes across the seagrass meadow is least effective during time periods of low canopy area, this may ultimately lead to seasonal increases in sediment resuspension during winter, as sediment suspension within the meadow was sensitive to wave oscillatory motion. Overall, at minimum frontal area in winter, average velocities were reduced, but the meadow behaved similarly to an unvegetated seafloor in regard to significant wave height, orbital velocities, and bottom shear stress. This agrees with findings from Bradley and Houser (2009) that attenuation of wave energy across a seagrass meadow is the result of the high density of seagrass blades and the aerial extent of the canopy, not the drag induced by flow interaction with individual blades.

Sediment Suspension

Overall, seasonal changes in the meadow frontal area strongly influenced wave development, bed shear stress, and subsequent sediment suspension in the seagrass meadow. During the summer, SSC at the unvegetated site was roughly double that within the seagrass canopy, while similar SSC were found in March and October within and outside the seagrass meadow. Many studies have also found that with increasing seagrass density, sediment resuspension is limited and sediment deposition occurs (Granata et al. 2001; Ward et al. 1984). Likely, this is caused by a transition from dense canopy cover during summer, where the canopy is essentially cutoff from the overflow, to a more sparse canopy cover, where the flow, vertical momentum, and mass transport is more vigorous (Luhar et al. 2008). In addition, under low canopy development in winter, although the magnitude of bottom shear was similar within the seagrass meadow and the adjacent unvegetated site, sediment suspension was enhanced within the meadow. This agrees with previous studies that have shown at low densities, seagrass enhanced sediment suspension through scouring (Bouma et al. 2009). Finer sediment

grain sizes were also found within the meadow, likely caused by enhanced deposition in summer. Since finer-grained particles typically resuspend at lower critical shear stresses than larger particles, this may have contributed to greater winter-time resuspension compared to unvegetated sites under similar bed shear stress conditions.

Although seasonal changes occur, Gacia and Duarte (2001) concluded that seagrass meadows often reduce resuspension rather than enhance deposition, as deposition only occurred during the summer and was only slightly increased. In yearly studies within a seagrass canopy undergoing restoration along the Virginia coast, turbidity levels during June–July, when the meadow was at peak biomass, showed significant reductions over a 10-year period with increased seagrass blade density and overall canopy size (Orth et al. 2012). *Z. marina* meadows also depend on seed production and germination in order to expand cover (Orth et al. 2006). Increased orbital motion, turbulence, and flow through the canopy can serve to distribute seeds in the spring (Orth et al. 2012), and the transport of seeds and other resources may be particularly important within the meadow's transition periods of senescence in the fall and growth in the spring/summer. During summer, flow reduction and sediment stabilization can serve to decrease turbidity and enhance the available light for photosynthesis (Carr et al. 2010, 2012), creating a positive feedback for seagrass growth.

Acknowledgments We thank A. Schwarzschild, C. Buck, B. Rodgers, and D. Boyd for field assistance, and J. Bricker for helpful discussions regarding wave–turbulence decomposition. This research was funded by the National Science Foundation (NSF-DEB 0621014, BSR-8702333-06, DEB-9211772, DEB-94118974, and DEB-0080381) to the Virginia Coast Reserve Long-Term Ecological Research program and by NSF-OCE 1151314. J.C.R. Hansen was supported through an NSF graduate research fellowship (DGE-0809128).

References

- Abdelrhman, M.A. 2003. Effect of eelgrass *Zostera marina* canopies on flow and transport. *Marine Ecology Progress Series* 248: 67–83.
- Ackerman, J.D., and A. Okubo. 1993. Reduced mixing in a marine macrophyte canopy. *Functional Ecology* 7: 305–309.
- Benilov, A.Y., and B.N. Filyushkin. 1970. Application of methods of linear filtration to an analysis of fluctuations in the surface layer of the sea. *Izvestiya, Atmospheric and Oceanic Physics* 6: 810–819.
- Bouma, T.J., M. Friedrichs, P. Klaassen, B.K. van Wesenbeek, F.G. Brun, S. Temmerman, M.M. van Katwijk, G. Graf, and P.M.J. Herman. 2009. Effects of shoot stiffness, shoot size and current velocity on scouring sediment from around seedlings and propagules. *Marine Ecology Progress Series* 388: 293–297.
- Bradley, K., and C. Houser. 2009. Relative velocity of seagrass blades: implications for wave attenuation in low-energy environments. *Journal of Geophysical Research* 114: F01004. doi:10.1029/2007JF000951.

- Bricker, J.D., and S.G. Monismith. 2007. Spectral wave-turbulence decomposition. *Journal of Atmospheric and Oceanic Technology* 24: 1479–1487.
- Bryan, K.R., H.W. Tay, C.A. Pilditch, C.J. Lundquist, and H.L. Hunt. 2007. The effects of seagrass (*Zostera muelleri*) on boundary-layer hydrodynamics in Whangapoua Estuary, New Zealand. *Journal of Coastal Research* SI50: 668–672.
- Carr, J., P. D'Odorico, K. McGlathery, and P. Wiberg. 2010. Stability and bistability of seagrass ecosystems in shallow coastal lagoons: role of feedbacks with sediment resuspension and light attenuation. *Journal of Geophysical Research* 115: G03011. doi:10.1029/2009JG001103.
- Carr, J.A., P. D'Odorico, K.J. McGlathery, and P.L. Wiberg. 2012. Modeling the effects of climate change on eelgrass stability and resilience: future scenarios and leading indicators of collapse. *Marine Ecology Progress Series* 448: 289–301.
- Chen, Q., H. Zhao, K. Ju, and S.L. Douglass. 2005. Prediction of wind waves in a shallow estuary. *Journal of Waterway, Port, Coastal, and Ocean Engineering* 131: 137–148.
- Chen, S., L.P. Sanford, E.W. Koch, F. Shi, and E.W. North. 2007. A nearshore model to investigate the effects of seagrass bed geometry on wave attenuation and suspended sediment transport. *Estuaries and Coasts* 30(2): 296–310.
- de Boer, W.F. 2007. Seagrass–sediment interactions, positive feedbacks and critical thresholds for occurrence: a review. *Hydrobiologia* 591: 5–24.
- Dean, R.G., and R.A. Dalrymple. 1991. *Water wave mechanics for engineers and scientists*. Singapore: World Scientific.
- Duarte, C.M. 1991. Seagrass depth limits. *Aquatic Botany* 40: 363–377.
- Fagherazzi, S., and P.L. Wiberg. 2009. Importance of wind conditions, fetch and water levels on wave-generated shear stresses in shallow intertidal basins. *Journal of Geophysical Research* 114: F03022. doi:10.1029/2008JF001139.
- Fonseca, M.S., and J.S. Fisher. 1986. A comparison of canopy friction and sediment movement between four species of seagrass with reference to their ecology and restoration. *Marine Ecology Progress Series* 29: 15–22.
- Fonseca, M.S., and M.A.R. Koehl. 2006. Flow in seagrass canopies: the influence of patch width. *Estuarine, Coastal and Shelf Science* 67: 1–9.
- Gacia, E., and C.M. Duarte. 2001. Sediment retention by a Mediterranean *Posidonia oceanica* meadow: the balance between deposition and resuspension. *Estuarine, Coastal and Shelf Science* 52: 505–514.
- Gacia, E., T.C. Granata, and C.M. Duarte. 1999. An approach to measurement of particle flux and sediment retention within seagrass (*Posidonia oceanica*) meadows. *Aquatic Botany* 65: 255–268.
- Gambi, M.C., A.R.M. Nowell, and P.A. Jumars. 1990. Flume observations on flow dynamics in *Zostera marina* (eelgrass) beds. *Marine Ecology Progress Series* 61: 159–169.
- Ghisalberti, M., and H. Nepf. 2006. The structure of the shear layer in flows over rigid and flexible canopies. *Environmental Fluid Mechanics* 6: 277–301.
- Granata, T.C., T. Serra, J. Colomer, X. Casamitjana, C.M. Duarte, and E. Gacia. 2001. Flow and particle distributions in a nearshore seagrass meadow before and after a storm. *Marine Ecology Progress Series* 218: 95–106.
- Grant, W.D., and O.S. Madsen. 1979. Combined wave and current interaction with a rough bottom. *Journal of Geophysical Research* 84: 1797–1808.
- Gruber, R.K., and W.M. Kemp. 2010. Feedback effects in a coastal canopy-forming submersed plant bed. *Limnology and Oceanography* 55(6): 2285–2298.
- Hansen, J.C.R., and M.A. Reidenbach. 2012. Wave and tidally driven flows in eelgrass beds and their effect on sediment suspension. *Marine Ecology Progress Series* 448: 271–287.
- Jing, L., and P.V. Ridd. 1996. Wave-current bottom shear stresses and sediment resuspension in Cleveland Bay, Australia. *Coastal Engineering* 29: 169–186.
- Kaimal, J., and J. Finnigan. 1994. *Atmospheric boundary layer flows: their structure and measurement*. New York: Oxford University Press.
- Koch, E.W., and G. Gust. 1999. Water flow in tide- and wave-dominated beds of the seagrass *Thalassia testudinum*. *Marine Ecology Progress Series* 184: 63–72.
- Koch, E.W., J.D. Ackerman, J. Verduin, and M. van Keulen. 2006. Fluid dynamics in seagrass ecology—from molecules to ecosystems. In *Seagrasses: biology, ecology and conservation*, ed. A.W.D. Larkum, R.J. Orth, and C. Duarte, 193–225. Amsterdam: Springer.
- Lacy, J.R., and S. Wyllie-Echeverria. 2011. The influence of current speed and vegetation density on flow structure in two macrotidal eelgrass canopies. *Limnology and Oceanography: Fluids and Environments* 1: 38–55.
- Lawson, S.E., P.L. Wiberg, K.J. McGlathery, and D.C. Fugate. 2007. Wind-driven sediment suspension controls light availability in a shallow coastal lagoon. *Estuaries and Coasts* 30(1): 102–112.
- Lawson, S.E., K.J. McGlathery, and P.L. Wiberg. 2012. Enhancement of sediment suspension and nutrient flux by benthic macrophytes at low biomass. *Marine Ecology Progress Series* 448: 259–270.
- Lowe, R.J., J.R. Koseff, and S.G. Monismith. 2005. Oscillatory flow through submerged canopies: 1. Velocity structure. *Journal of Geophysical Research* 110: C10016. doi:10.1029/2004JC002788.
- Lu, S.S., and W.W. Willmarth. 1973. Measurements of the structure of the Reynolds stress in a turbulent boundary layer. *Journal of Fluid Mechanics* 60: 481–571.
- Luhar, M., J. Rominger, and H. Nepf. 2008. Interaction between flow, transport and vegetation spatial structure. *Environmental Fluid Mechanics* 8: 423–439.
- Luhar, M., S. Coutu, E. Infantes, S. Fox, and H. Nepf. 2010. Wave-induced velocities inside a model seagrass bed. *Journal of Geophysical Research* 115: C12005. doi:10.1029/2010JC006345.
- McGlathery, K., I.C. Anderson, and A.C. Tyler. 2001. Magnitude and variability of benthic and pelagic metabolism in a temperate coastal lagoon. *Marine Ecology Progress Series* 216: 1–15.
- Moore, K.A., R.J. Orth, and J.F. Nowak. 1993. Environmental regulation of seed germination in *Zostera marina* L. (eelgrass) in Chesapeake Bay: effects of light, oxygen and sediment burial. *Aquatic Botany* 45: 79–91.
- Nepf, H.M. 1999. Drag, turbulence, and diffusion in flow through emergent vegetation. *Water Resources Research* 35(2): 479–489.
- Nepf, H.M. 2012. Flow and transport in regions with aquatic vegetation. *Annual Review of Fluid Mechanics* 44: 123–142.
- Nepf, H.M., J.A. Sullivan, and R.A. Zavistoski. 1997. A model for diffusion within emergent vegetation. *Limnology and Oceanography* 42(8): 1735–1745.
- Nepf, H., M. Ghisalberti, B. White, and E. Murphy. 2007. Retention time and dispersion associated with submerged aquatic canopies. *Water Resources Research* 43: W04422. doi:10.1029/2006WR005362.
- Orth, R.J., and K.J. McGlathery. 2012. Eelgrass recovery in the coastal bays of the Virginia Coast Reserve, USA. *Marine Ecology Progress Series* 448: 173–176.
- Orth, R.J., M.L. Luckenbach, S.R. Marion, K.A. Moore, and D.J. Wilcox. 2006. Seagrass recovery in the Delmarva Coastal Bays, USA. *Aquatic Botany* 84: 26–36.
- Orth, R.J., K.A. Moore, S.R. Marion, D. Wilcox, and D. Parrish. 2012. Seed addition facilitates *Zostera marina* L. (eelgrass) recovery in a coastal bay system (USA). *Marine Ecology Progress Series* 448: 177–195.
- Peterson, C.H., R.A. Luettich Jr., M. Fiorenza, and G.A. Skilleter. 2004. Attenuation of water flow inside seagrass canopies of

- differing structure. *Marine Ecology Progress Series* 268: 81–92.
- Raupach, M.R., J.J. Finnigan, and Y. Brunet. 1996. Coherent eddies and turbulence in vegetation canopies: the mixing-layer analogy. *Boundary-Layer Meteorology* 78: 351–382.
- Sand-Jensen, K. 2008. Drag forces on common plant species in temperate streams: consequences of morphology, velocity and biomass. *Hydrobiologia* 610(1): 307–319.
- Stapleton, K.R., and D.A. Huntley. 1995. Seabed stress determinations using the inertial dissipation method and the turbulent kinetic energy method. *Earth Surface Processes and Landforms* 20: 807–815.
- Trowbridge, J.H. 1998. On a technique for measurement of turbulent shear stress in the presence of surface waves. *Journal of Atmospheric and Oceanic Technology* 15: 290–298.
- Verduin, J.J., and J.O. Backhaus. 2000. Dynamics of plant–flow interactions for the seagrass *Amphibolis antarctica*: field observations and model simulations. *Estuarine, Coastal and Shelf Science* 50: 185–204.
- Vogel, S. 1981. *Life in moving fluids*. Boston: Grant.
- Ward, L.G., W.M. Kemp, and W.R. Boynton. 1984. The influence of waves and seagrass communities on suspended particulates in an estuarine embayment. *Marine Geology* 59: 85–103.
- Wiberg, P.L., and C.R. Sherwood. 2008. Calculating wave-generated bottom orbital velocities from surface-wave parameters. *Computer and Geosciences* 34: 1243–1262.
- Wiberg, P.L., and J.D. Smith. 1983. A comparison of field data and theoretical models for wave current interactions at the bed on the continental shelf. *Continental Shelf Research* 2: 147–162.
- Widdows, J., N.D. Pope, M.D. Brinsley, H. Asmus, and R.M. Asmus. 2008. Effects of seagrass beds (*Zostera noltii* and *Z. marina*) on near-bed hydrodynamics and sediment resuspension. *Marine Ecology Progress Series* 358: 125–136.